Sensors and Actuators B 253 (2017) 584–591

Contents lists available at ScienceDirect

Sensors and Actuators B: Chemical

journal homepage: www.elsevier.com/locate/snb

One-pot synthesis of In doped NiO nanofibers and their gas sensing properties

Changhao Feng [a,b,*], Xueying Kou [c], Bin Chen [a,b], Guobing Qian [a,b], Yanfeng Sun [c,**], Geyu Lu [c]

[a] College of Electronic and Information Engineering, Southwest University, Chongqing 400715, China
[b] Chongqing Key Laboratory of Nonlinear Circuits and Intelligent Information Processing, Chongqing 400715, China
[c] State Key Laboratory on Integrated Optoelectronics, College of Electronic Science and Engineering, Jilin University, Changchun 130012, China

ARTICLE INFO

Article history:
Received 22 March 2017
Received in revised form 14 June 2017
Accepted 16 June 2017
Available online 26 June 2017

Keywords:
In-doped NiO nanofibers
Electrospinning
Methanol
Gas sensor

ABSTRACT

A series of In-doped NiO nanofibers have been synthesized by electrospinning method in this paper, and the gas sensing properties of nanofibers to methanol were investigated. Due to the concentration reduce of carrier, the In-doped NiO nanofibers show good sensing properties to methanol. At the optimal operating temperature of 300 °C, the response of In-doped NiO nanofibers to 200 ppm methanol is 10.9, which is almost 5.2 times higher than that of pure NiO nanofibers. These gas sensing results indicate In-doped NiO nanofibers exhibit good selectivity, repeatability and long term stability characteristics, which means In-doped NiO nanofibers to be the promising candidates for detect methanol vapor in air.

1. Introduction

Methanol (CH_3OH) is a highly volatile and flammable liquid, which is widely used to manufacture biodiesel, antifreeze, dyes, paints, perfume etc. However, methanol has strong toxicity to human health, especially to optic nerve, retina and blood system [1–5]. Compared to formaldehyde, ethanol, and toluene, there are few researches on methanol sensing properties. Therefore, it is of great significance to study and develop a high response, reliable, cost-effective, portable, and selective methanol sensor. For above mentioned reasons, gas sensors, especially based on MOS (Metal Oxide Semiconductor), have attracted great attention in detection of harmful, environmental, explosive and toxic gas [6–8]. This kind of gas sensor inform about composition of ambient atmosphere through conductivity changes of semiconductor, such as SnO_2 [9–11], In_2O_3 [12–14], WO_3 [15–17], Fe_2O_3 [18,19] and NiO [20–22]. However, designing high performance methanol sensors based on MOS is still in the early stage.

Nickel oxide (NiO) with p-type semiconducting properties (Eg = 3.6–4.0 eV) under ambient conditions. Due to benefits of relative wide band gap, high specific surface areas, excellent structural stability, higher amount of oxygen adsorption and outstanding transportation properties, NiO has been extensively investigated in a number of fields, such as catalysis [23], electrodes [24,25], supercapacitors [26,27] and magnetic materials [28]. By preparing NiO with different morphologies [29,30], loading noble metal or noble metal oxide catalysts [12,31] and doping aliovalent metal oxides [32], high sensing performance nano-materials were designed. For example, Jong-Heun Le et al. have synthesized thin walled NiO tubes functionalized by catalytic Pt via nanofiber templating and multilayered sputter-coating, these Pt-NiO-Pt nanotubes exhibited superior C_2H_5OH sensing response [20]. Il-Doo Kim et al. have fabricated NiO arrays with a hollow hemisphere by colloidal templating and RF-sputtering, which shows enhanced responses to C_2H_5OH [22]. Taihong Wang et al. have prepared plate-like heterogeneous NiO/WO_3 nanocomposites, which show excellent sensitivity towards NO_2 and ultrafast response even at room temperature [33]. These results indicate that NiO is a promising candidate for highly sensitive and selective gas sensors. In_2O_3, as a kind of important sensing material, has been widely used to detect NO_2, NO, C_2H_5OH, and CH_3OH. However, most of reports are focused on gas sensing properties of NiO or In_2O_3, little attention has been given to methanol-sensing properties of In-doped NiO 1D nano-materials.

In this paper, we developed a facile strategy to prepare a series of methanol sensors fabricated by In-doped NiO nanofibers. Furthermore, gas sensing properties of those nanofibers were investigated. A comparative gas sensing study between pure and In-doped NiO nanofibers was performed. These results indicate In-doped

* Corresponding author at: College of Electronic and Information Engineering, Southwest University, Chongqing 400715, China
** Corresponding author.
E-mail addresses: fengchanghao@qq.com (C. Feng), syf@jlu.edu.cn (Y. Sun).

http://dx.doi.org/10.1016/j.snb.2017.06.115
0925-4005/

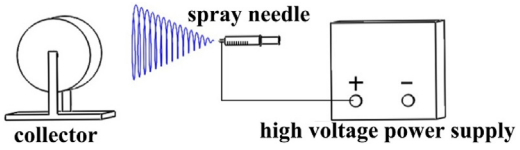

Fig 1. Schematic illustration of electrospinning apparatus.

nanofibers (especially molar ratio of In^{3+}:Ni^{2+} is 3:100) show outstanding sensing properties toward methanol with enhanced response, selective and repeatability characteristics. At last, the effect of In doping was investigated and a possible mechanism is proposed.

2. Experimental section

2.1. Perparation of pure and In-doped NiO nanofibers

All chemicals used were analytic grade reagents without further purification. Pure and In-doped NiO nanofibers were synthesized by electrospinning method. Polyvinyl pyrrolidone (PVP, K90) and *N,N*-Dimethylformamide (DMF) were purchased from Sinopharm-Aldrich, USA. Indium nitrate ($In(NO_3)_3$), nickel chloride ($NiCl_2$) and absolute ethanol (C_2H_5OH) were purchased from Beijing Chemicals Co., Ltd, China.

The In-doped NiO nanofibers with various dopant concentrations were synthesized by electrospinning. The ratios of In^{3+} to Ni^{2+} in nanofibers are 0, 1.5, 3 and 6 mol%, which were labeled as S1, S2, S3 and S4, respectively. In a typical procedure for preparing In-doped nanofibers precursor solution with a molar ratio of 1.5:100, 2 mmol $NiCl_2$ and 0.03 mmol $In(NO_3)_3$ were dissolved in a mixture of DMF and ethanol, and stirring for 15 min. Then PVP was added into above solutions with magnetic stirring for 3 h at 50 °C, until a viscous precursor solutions completely formed. The electrospinning precursor solutions of pure NiO, In-doped NiO nanofibers with a molar ratio of 3:100 and 6:100 were made by using same reagents except with different amount of $In(NO_3)_3$. After fully stirring, the precursor solutions were transferred into electrospinning installation. Fig. 1 is schematic diagram of electrospinning installation, which consists of three major components: high-voltage power supply, collector, and spinneret. The inner diameter of spinneret was 1.01 mm, voltage between spinneret and collector was 10–13 kV, and distance between spinneret and collector was 10 cm. The flow rate of precursor solution was fixed at 0.3 mL/h by using KD Scientific syringe pump. In order to decomposing PVP completely, as-synthesized nanofibers were calcined at 500 °C for 3 h in air, and the heating ratio was 1 °C/min.

The X-ray diffraction (XRD) patterns were recorded by a Rigaku TTRIII X-ray diffractometer with Cu-Kα1 radiation (λ = 0.15406 nm) in the range of 20–80° (2θ) at room temperature. Field emission scanning electron microscopy (FESEM) images were obtained using a JEOL JSM-7500F microscope with an acceleration voltage of 15 kV. The energy-dispersive X-ray spectroscopy (EDX) spots pattern scanning analysis was performed by the TEM attachment. Transmission electron microscopic (TEM) and high-resolution transmission electron microscopic (HRTEM) images, and selected area electron diffractive (SAED) patterns were obtained on a JEOL JEM-3010 transmission electron microscope with an acceleration voltage of 200 kV.

2.2. Fabrication and measurement of gas sensor

Fig. 2a and b are photographs of substrate. The size of Al_2O_3 substrate is 1.0 mm × 1.5 mm. With two L golden electrodes on the front side, and ruthenium oxides (RuO_2) layer is made on the back side as a micro-heater by screen printing technique. And there are two Au electrodes on the RuO2 heating layer to supply current. Each electrode was connected with Pt wire. The operating temperature was controlled by adjusting the current that passed through the micro-heater. The temperature distributes uniformity on the substrate, as shown in Fig. S1. The temperature of substrate is about 300 °C. And the emissivity value used to record the micro-heater temperature of FLIR is fixed on 0.9. The working temperatures were controlled by micro-heater which was measured using an FLIR temperature sensor. The power consumptions 90.3, 102.1, 116.9, 129.8, 150.5, 165 and 188.5 mW are used to heat the substrates to 225, 250, 275, 300, 325, 350 and 375 °C, respectively. The In-doped NiO nanofibers were pressed on substrate mildly by Hot Press Machine (HS-XX40, Hesen Inc., China) at 120 °C for 5 min. By doing this, sensing materials made a good contact to electrodes. The gas sensing properties of In-doped NiO nanofibers were measured by static testing method, as diagrammed in our previous works [6,34]: First, gas sensors were put into gas chamber which filled with fresh air, and a given amount of test VOCs were injected into gas chamber by using a micro-injector, and the concentrations of VOCs were obtained by static liquid gas distribution method [35], which was calculated by Formula (1).

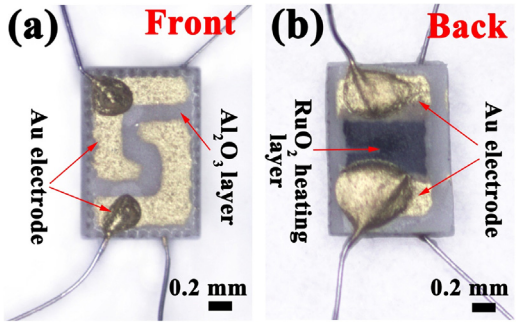

Fig. 2. Schematic structure of the alumina substrate.

$$C = \frac{22.4 \times \varphi \times \rho \times V_1}{M \times V_2} \quad (1)$$

where C (ppm) is concentration of VOCs, φ is volume fraction of VOCs, ρ (g/mL) is density of VOCs, V_1 (μL) is volume of VOCs, V_2 (L) is volume of chamber and M (g/mol) is molecular weight of VOCs. Gas sensing properties of nanofibers were tested under same condition: the relative humidity is 25–35%, and the temperature is 20–25 °C. The response of gas sensor was defined as the ratio of resistance in air to that in tested gas. Response and recovery time were defined as the time taken by sensors achieve 90% of total resistance change in the case of adsorption and desorption, respectively [35].

3. Results and discussion

XRD patterns of nanofibers are shown in Fig. 3, the crystal phase of sample S1 is NiO, and all the diffraction peaks can be indexed to the pure cubic structure of NiO (JCPDS # 47-1049). No other phase corresponding to indium compound was observed in the XRD patterns of S2, S3 and S4 nanomaterials. The average crystal size of nanofibers S1, S2, S3 and S4 were ~21.1 nm, 20.2 nm, 18.0 nm and 16.8 nm. And the crystallinity of nanofibers decreases with doping, this is because the excess of In acting as a grain growth inhibitor not allowing the crystallite size to increase, which is according with the researchs of S. Ruan [36]. What's more, the radius of In^{3+} is 0.08 nm, which is higher than that of Ni^{2+} (0.069 nm) at a coordination number (CN) of 6. Therefore, diffraction peaks evidently shift to left with increase the doping amount of In. Fig. 3b clearly showed that there was a 0.13° right shift in (111) and (200) diffraction peaks

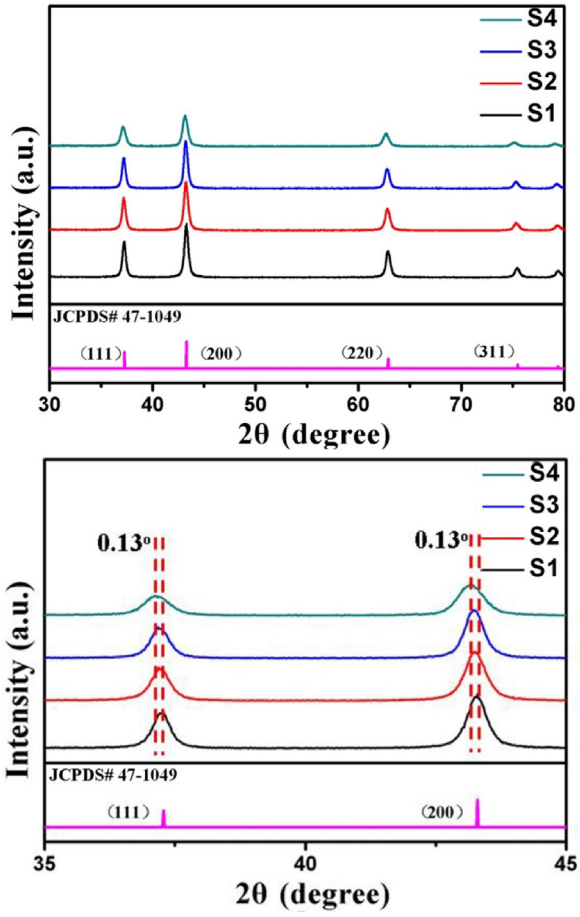

Fig. 3. (a) XRD patterns of In-NiO nanofibers with sample S1, S2, S3 and S4, (b) Comparison of (111) and (200) peaks from XRD patterns.

of nanofibers S4 compared with S1. The results indicate In^{3+} could enter NiO lattice by this method.

The morphology and microstructure of nanofibers S1, S2, S3 and S4 were confirmed by FESEM and TEM. As shown in Fig. S2, the diameters of nanofibers are decrease after calcined. The diameter of precursor nanofiber S1 is ~140 nm, and the diameter of nanofiber after calcined S1 is ~80 nm. As shown in Fig. 4, all nanofibers had rough and porous surfaces and have a diameter of ~80 nm. The porous nanofibers are composed by many small nanoparticles, and this gas accessible nanostructure is advantageous for enhancing gas responding kinetics [37]. To further study internal structure of nanofibers, TEM, HRTEM and EDS were employed. As Fig. 5a shows, the morphology of nanofibers S3 in TEM images are similar to that of FESEM. Fig. 5b shows HRTEM images which obtained from the marked circles in Fig. 5a. The lattice fringes could be clearly observed and lattice spacing are 0.241 nm and 0.209 nm, which corresponding to (111) and (100) planes of NiO, respectively. Fig. 5b–e depicts the elemental composition and spatial distribution of Ni, In and O in the nanofibers S3, the distribution of In element is uniform in the nanofibers. And the peaks of Ni, In and O can be clearly seen in Fig. 5f. Therefore, it clearly shows that In doped into NiO lattice.

It is well known the response of gas sensors based on metal oxides is greatly influenced by operating temperature. In order to determine the optimum operating temperatures of sensors S1, S2, S3, and S4, the responses of sensors S1, S2, S3, and S4 to 200 ppm methanol were tested as a function of operating temperature as shown in Fig. 6. It can be seen that sensors S1 and S2 have the maximum responses at 325 °C, while sensors S3 and S4 have the maximum responses at 300 °C and 275 °C, respectively. Obviously, there were shifts of optimal operating temperatures among sensors by increase the doping amount of In. And sensors S3 showed the highest response towards 200 ppm methanol, which is almost 5.2 times higher than that of sensor S1. As a result, 300 °C was selected as the operating temperature for sensors S3 in the following gas testing process. The results of methanol sensing properties compared to other metal-oxide nanostructures are show in Table 1. There are various gas sensing materials were used to detect methanol [38–43], including n-type and p-type oxide semiconductors, such as ZnO, In_2O_3, SnO_2, CuO and so on. The gas response in this work is higher than that of works mentioned above, with a moderate operating temperature. As shown in Fig. 6b, the resistance in air is increase with doping amount increase. The resistance in air of S1, S2, S3 and S4 are 5.1, 10.5, 29.5 and 39.8 kΩ at 300 °C. And the activation energy (E) of nanofiber S1, S2, S3 and S4 are 7.777×10^{-20} J, 1.319×10^{-19} J, 1.348×10^{-19} J and 1.357×10^{-19} J, which were calculated by Formula (2) and (3).

$$b = \frac{InR_{T1} - InR_{T2}}{\left(\frac{1}{T_1} - \frac{1}{T_2}\right)} \quad (2)$$

$$E = bk \quad (3)$$

Where T_1 and T_2 are thermodynamic temperature, R_{T1} and R_{T2} are the resistance at T_1 and T_2, k is Boltzmann constant ($k = 1.38 \times 10^{-23}$ J/K).

Fig. 7 reveals the gas response of sensors S1 and S3 as a function of methanol concentrations at the optimum operating temperature. The results indicate that responses of two kinds of sensors both increased with methanol concentration from 15 to 500 ppm. The response of sensors S3 is 17.28 for 500 ppm methanol vapor and detection limit is 15 ppm with a response of 2.26. And the response

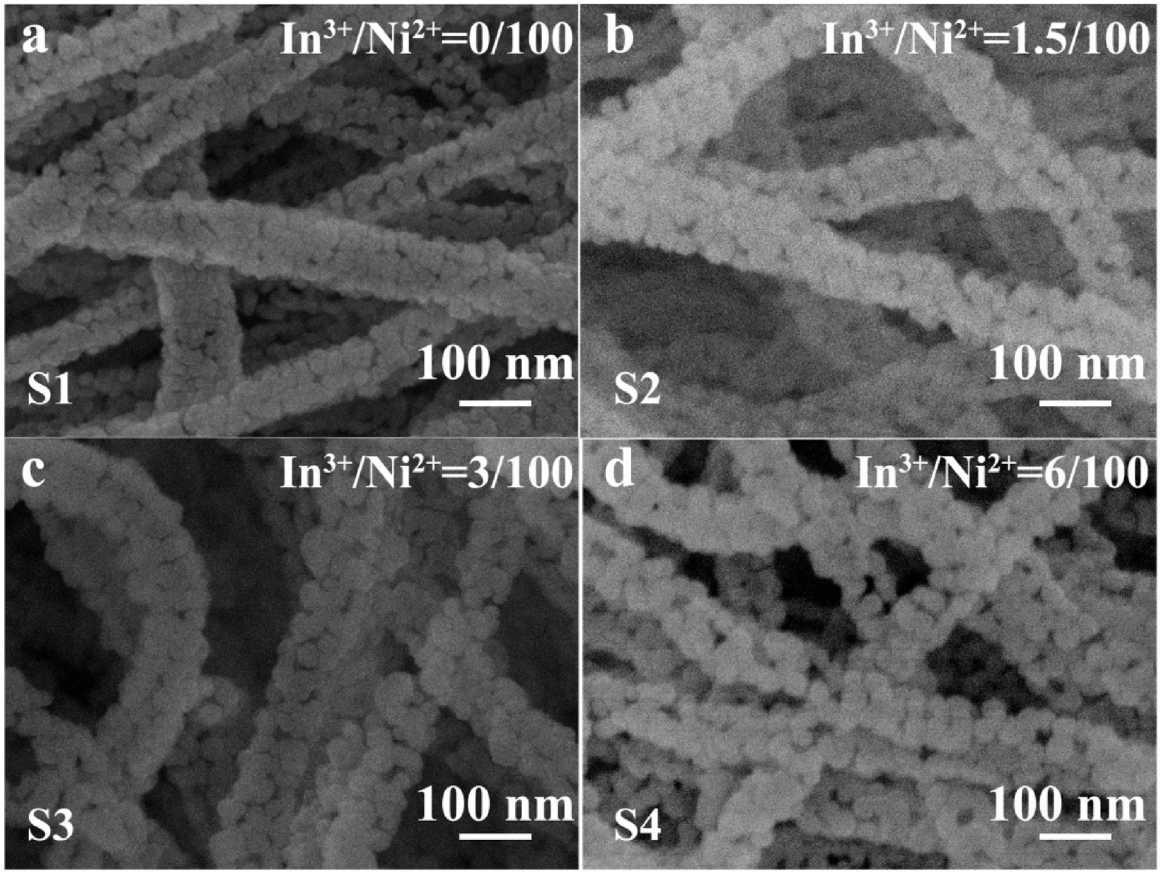

Fig. 4. FESEM images of sample (a) S1, (b) S2, (c) S3, (d) S4.

Table 1
Comparison of methanol gas sensors based on metal oxide nanostructures.

Materials	Operating temperature	Methanol Concentration	Response	Response time	Recovery time	Ref.
ZnO nanorods	300 °C	100 ppm	3.11	216 s	405 s	[38]
ZnO thin film	275 °C	500 ppm	17	280 s	135 s	[39]
flower-like In_2O_3 microrods	300 °C	100 ppm	3	15 s	20 s	[40]
CdS-doped SnO_2 thick films	200 °C	5000 ppm	70	90 s	200 s	[41]
ZnO/SnO2 nanostructure	300 °C	100 ppm	9.6	10 s	10 s	[42]
CuO thin film	350 °C	500 ppm	1.12	235 s	225 s	[43]
In-doped NiO nanotubes	300 °C	200 ppm	10.9	273 s	26 s	This work

of sensors S1 is 2.1 for 500 ppm methanol and detection limit is 25 ppm with a response of 1.14. Obviously, sensors based on In-doped NiO nanofibers exhibited an enhanced response to methanol compared with pure NiO.

Fig. 8 shows transient and dynamic characteristics of sensors S3. It can be seen that sensors S3 showed sensitive and reversible response to methanol. The transient characteristics of sensors S3 in 200 ppm methanol are shown in Panels a, we can see that recovery time is about 26 s, which indicates sensors S3 exhibit fast recovery procedure at 300 °C. In addition, sensor S3 exhibit excellent reproducibility as shown in the inset of Fig. 8a. There are four reversible cycles of response curve without a clear decrease for 200 ppm methanol, which indicates the good repeatable characteristics of sensors S3. Fig. 8b shows the dynamic characteristics of sensors S3, which were orderly exposed to 15, 25, 50, 100, 200, and 300 ppm methanol at 300 °C, and the responses were approximately 2.21, 3.54, 5.04, 6.61, 10.9, and 16.45, respectively.

The responses of sensor S1 and S3 to 200 ppm various testing gases are shown in Fig. 9. Six kinds of gases were tested, including methanol, ethanol, acetone, formaldehyde, benzene, and xylene. It can be seen that sensors S3 displayed enhanced response by compare with sensor S1. The responses of sensor S1 did not show any significant selectivity to a specific gas, whereas sensors S3 exhibit highest response to methanol among these tested gas, and the response to 200 ppm methanol is about 10.9, while the responses to other gases are much lower, which revealed an good selectivity to methanol opposed to other gases at the same concentrations.

The long term stability experiment of sensor S3 to 200 ppm methanol was carried out over 30 days. As displayed in Fig. 10, the response values were decrease from 10.9 to 8.7 after 30 days. It is probably because the nanofibers contain many grain boundaries, the response degraded a little for long term measurement.

NiO and In doped NiO show typical gas-sensing properties of p-type semiconductor. The sensing mechanism of p-type semiconductor is primarily caused by adsorption and desorption of target gas molecular on the surface of sensing material. Oxygen molecules chemisorbed and dissociated on the surface of sensing material, and generate oxygen species (O_2^-,O^-,O^{2-}). The holes will move to the surfaces through electrostatic interaction, and form a hole accumulation layers (HAL), which result in an decrease in the resis-

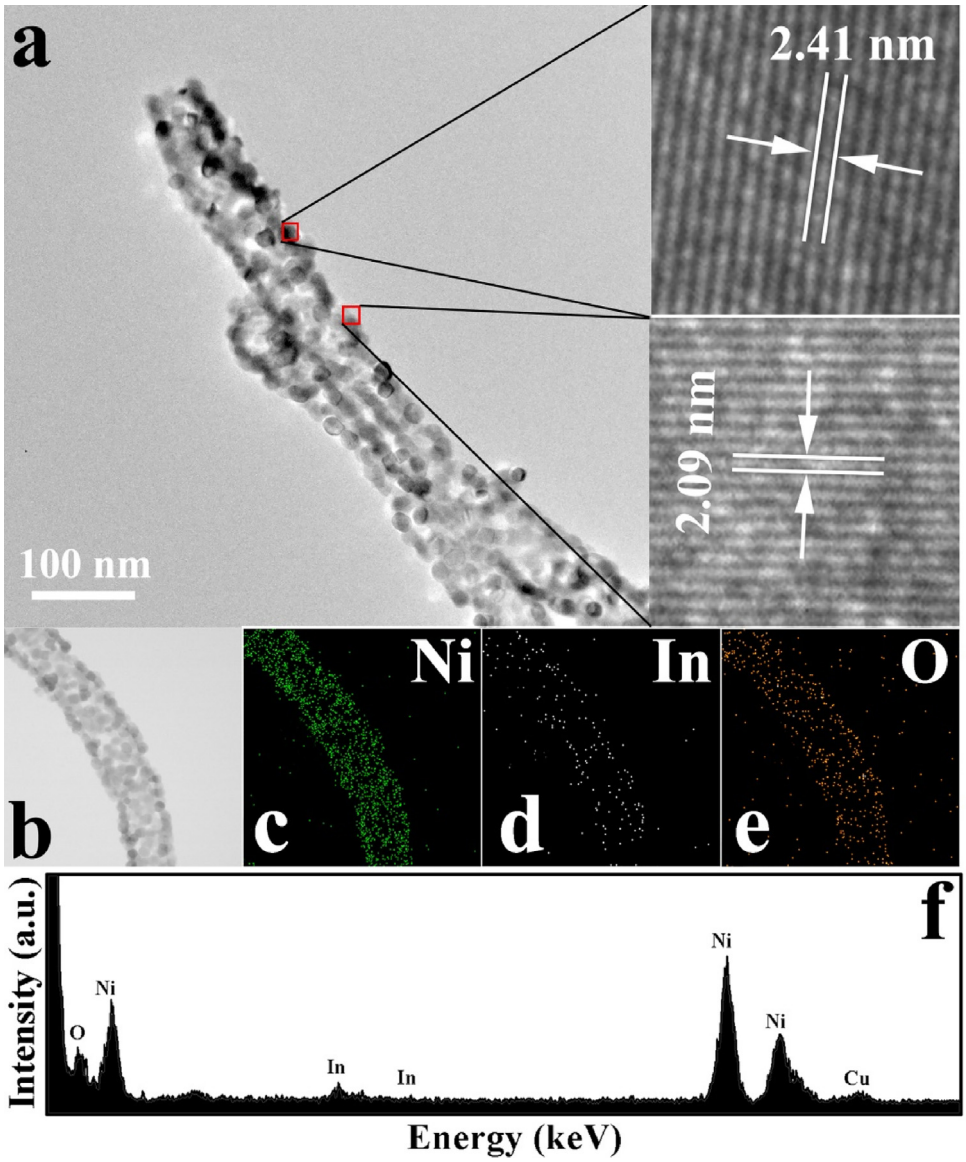

Fig. 5. (a) TEM images pattern of the nanofibers S4. The insets are the HRTEM images of selected areas. (b)–(e) are EDS elemental maps and (f) is spots pattern of In, Ni and O.

tance [21,31]. Methanol is a reducing VOCs, which can react with adsorbed oxygen and release electrons back to conduction band, leading to an increase in the resistance. The reaction near the surface can be simply written as follow.

$$O_2\,(gas) \leftrightarrow O_2\,(ads) \tag{4}$$

$$O_2\,(ads) + e^- \rightarrow O_2^- \tag{5}$$

$$O_2^- + e^- \rightarrow 2O^- \tag{6}$$

$$2O^- + e^- \rightarrow O^{2-} \tag{7}$$

$$CH_3OH + O_2^- \rightarrow HCOOH + H_2O + e^- \tag{8}$$

$$CH_3OH + O^- \rightarrow HCHO + H_2O + e^- \tag{9}$$

What's more, the concentration change of holes may be a key factor for enhance gas sensing properties by In-doped NiO nanofibers. According to previous research by Hyo-Joong Kim et al. [44], gas response of p type semiconductor can be written as follows:

$$S = \frac{R_g}{R_a} = \frac{p_a}{p_g} = \frac{p_a}{p_a - \Delta p} = \frac{\Delta p}{(p_a - \Delta p)} + 1 \tag{10}$$

where R_a and R_g are resistance in air and target gas, p_a and p_g are hole concentrations in air and target gas, and $\Delta p = p_a - p_g$ is concentration variation of hole on exposure to target gas. Accordingly, a higher response can be got when hole concentration in air (p_a) becomes lower [21]. In this paper, the responses of sensor S2, S3 and S4 to methanol were found to be higher than that of pure NiO nanofibers should be ascribed to lower concentration of holes. When hole concentration is lower, gas sensing reaction will lead to a higher variation in resistance, the resistances in air of S1, S2 and S3 are 5.1, 10.5 and 29.5 kΩ at 300 °C, with the response of S1, S2 and S3 to 200 ppm methanol are 1.8, 4.5 and 10.9, and this phenomenon has previously been confirmed by our previous research NiO [34]. What's more, with the increment of In doping amount, the morphology of nanofibers changed. However, when the molar ratio of In^{3+}/Ni^{2+} increased to 6%, excessive In doping will lead the surface of sensing body covered by more In ions. And the atom ratio of In3d to Ni2p in S2, S3 and S4 are 2.9%, 3.8% and 9.1%, which is confirmed by the result of XPS. Therefore, the active sites and response will become decrease. For this reason, the response of sensors S4 is lower than sensors S3. Further study and systematic

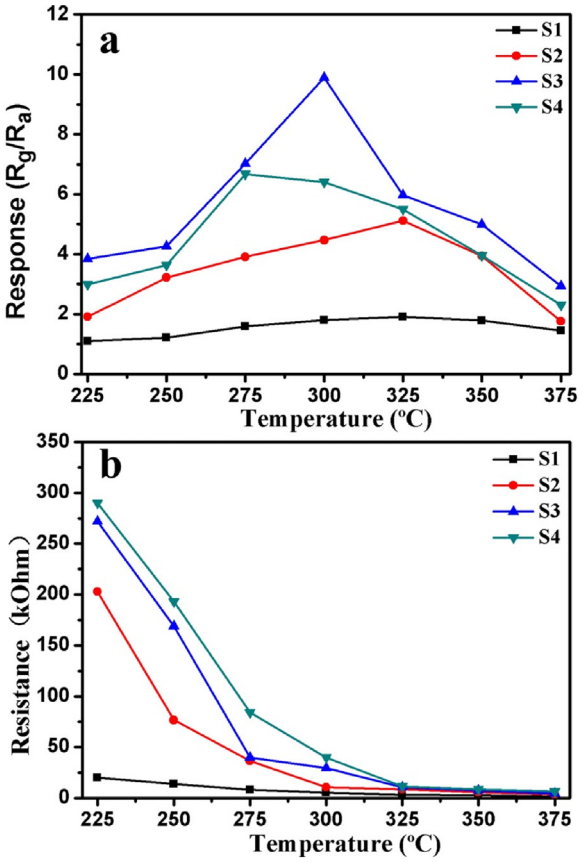

Fig. 6. (a) Response of sensors based on S1, S2, S3 and S4 nanofibers to 200 ppm methanol as function of the operating temperature. (b) The resistance of samples in air as function of the operating temperature.

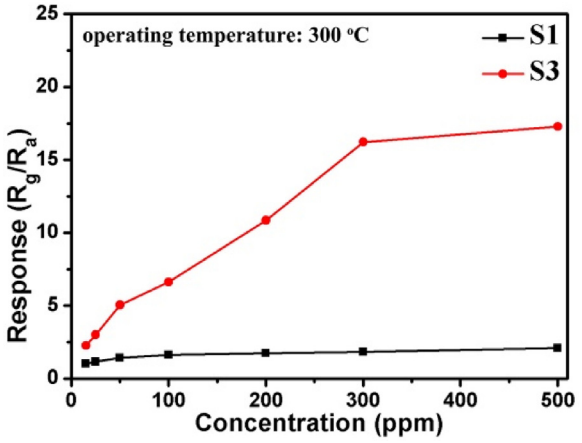

Fig. 7. Response of sensors based on nanofibers S1 and S3 toward methanol at different concentrations.

experiments are needed for deep understanding of In-doped NiO nanofibers induced sensing properties, which is now in progress.

4. Conclusion

In summary, a series of pure NiO and In doped-NiO nanofibers have been synthesized through a simple and facile electrospinning technique. The results of characterization indicate that nanofibers with In^{3+}/Ni^{2+} = 3 mol% demonstrate significantly enhanced response to methanol compared with other counterpart. The gas sensors based on nanofibers S3 demonstrated good

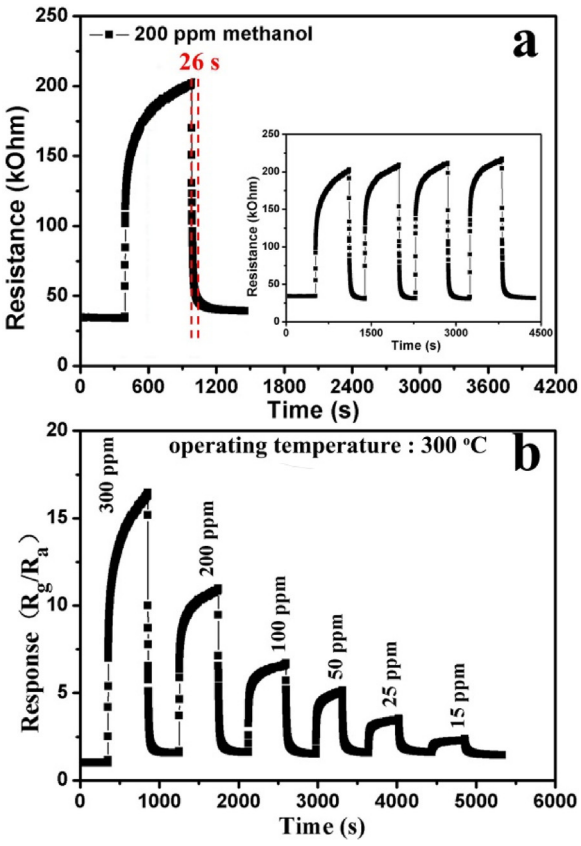

Fig. 8. (a) is the dynamic response of sensor based on nanofibers S3 to 200 ppm methanol. (b) is the response and recovery curves of the sensor S3 to different concentrations of methanol at the operating temperature.

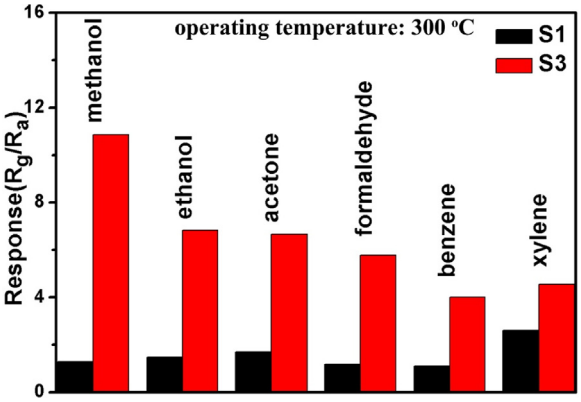

Fig. 9. Comparison in the response of sensor S1 and S3 to 200 ppm different gas.

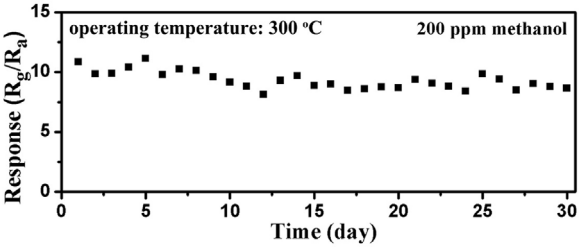

Fig. 10. Long-term stability of sensor S3 at the operating temperature.

selectivity, repeatability and long term stability at the optimum temperature. The method by modulating the density of hole in NiO nanofibers provides a new and promising strategy to design high performance methanol sensor. The good methanol sensing characteristic indicates that sensors based on In-doped NiO nanofibers are promising for methanol sensors which used by air-quality and environmental monitoring.

Acknowledgements

This work is supported by the Fundamental Research Funds for the Central Universities under Grant numbers XDJK2017C074, SWU116059 and SWU116013, China Postdoctoral Science Foundation (No. 2016M602631 and 2017M610583), National Nature Science Foundation of China (No. 61134010, 61304242, 61327804, 61377058 and 61374218), Program for Chang Jiang Scholars and Innovative Research Team in University (No. IRT13018).

Appendix A. Supplementary data

Supplementary data associated with this article can be found, in the online version, at **http://dx.doi.org/10.1016/j.snb.2017.06.115**.

References

[1] Q. Zhu, Y.M. Zhang, J. Zhang, Z.Q. Zhu, Q.J. Liu, A new and high response gas sensor for methanol using molecularly imprinted technique, Sens. Actuators B 207 (2015) 398–403.
[2] D. Han, P. Song, S. Zhang, H. Zhang, Q. Xu, Q. Wang, Enhanced methanol gas-sensing performance of Ce-doped In_2O_3 porous nanospheres prepared by hydrothermal method, Sens. Actuators B 216 (2015) 488–496.
[3] W. Tang, J. Wang, P. Yao, X. Li, Hollow hierarchical SnO_2-ZnO composite nanofibers with heterostructure based on electrospinning method for detecting methanol, Sens. Actuators B 192 (2014) 543–549.
[4] M. Babaei, N. Alizadeh, Methanol selective gas sensor based on nano-structured conducting polypyrrole prepared by electrochemically on interdigital electrodes for biodiesel analysis, Sens. Actuators B 183 (2013) 617–626.
[5] Q. Zhu, Y.M. Zhang, J. Zhang, Z.Q. Zhu, Q.J. Liu, Hybrid 3D structures of ZnO nanoflowers and PdO nanoparticles as a highly selective methanol sensor, Analyst 141 (2016) 2977–2989.
[6] C. Feng, X. Li, J. Ma, Y. Sun, C. Wang, P. Sun, J. Zheng, G. Lu, Facile synthesis and gas sensing properties of In_2O_3-WO_3 heterojunction nanofibers, Sens. Actuators B 209 (2015) 622–629.
[7] C. Wang, X. Cheng, X. Zhou, P. Sun, X. Hu, K. Shimanoe, G. Lu, N. Yamazoe, Hierarchical α-Fe_2O_3/NiO composites with a hollow structure for a gas sensor, ACS Appl. Mater. Interfaces 6 (2014) 12031–12037.
[8] X. Zhou, J. Liu, C. Wang, P. Sun, X. Hu, X. Li, K. Shimanoe, N. Yamazoe, G. Lu, Highly sensitive acetone gas sensor based on porous $ZnFe_2O_4$ nanospheres, Sens. Actuators B 206 (2015) 577–583.
[9] N. Yamazoe, New approaches for improving semiconductor gas sensors, Sens. Actuators B 5 (2010) 7–19.
[10] P. Sun, X. Zhou, C. Wang, B. Wang, X. Xu, G. Lu, One-step synthesis and gas sensing properties of hierarchical Cd-doped SnO_2 nanostructures, Sens. Actuators B 190 (2014) 32–39.
[11] Y. Choi, I. Hwang, J. Park, K. Choi, J. Park, J. Lee, Novel fabrication of an SnO_2 nanowire gas sensor with high sensitivity, Nanotechnology 19 (2008) 095508.
[12] P. Rai, J. Yoon, C. Kwak, J. Lee, Role of Pd nanoparticles in gas sensing behaviour of Pd@In_2O_3 yolk-shell nanoreactors, J. Mater. Chem. A 4 (2016) 264–269.
[13] A. Gurlo, N. Bârsan, M. Ivanovskaya, U. Weimar, W. Göpel, In_2O_3 and MoO_3-In_2O_3 thin film semiconductor sensors: interaction with NO_2 and O_3, Sens. Actuators B 47 (1998) 92–99.
[14] J. Tamaki, C. Naruo, Y. Yamamoto, M. Matsuoka, Sensing properties to dilute chlorine gas of indium oxide based thin film sensors prepared by electron beam evaporation, Sens. Actuators B 83 (2002) 190–194.
[15] C. Lee, S. Kim, I. Hwang, J. Lee, Glucose-mediated hydrothermal synthesis and gas sensing characteristics of WO_3 hollow microspheres, Sens. Actuators B 142 (2009) 236–242.
[16] J. Kim, J. Yoon, Y. Hong, Y. Kang, F. Abdel-Hady, A. Wazzan, J. Lee, Highly sensitive and selective detection of ppb-level NO_2 using multi-shelled WO_3 yolk-shell spheres, Sens. Actuators B 229 (2016) 561–569.
[17] C. Wang, X. Li, C. Feng, Y. Sun, G. Lu, Nanosheets assembled hierarchical flower-like WO_3 nanostructures: synthesis, characterization, and their gas sensing properties, Sens. Actuators B 210 (2015) 75–81.
[18] X. Hu, J. Yu, J. Gong, Q. Li, G. Li, α-Fe_2O_3 nanorings prepared by a microwave-assisted hydrothermal process and their sensing properties, Adv. Mater. 19 (2007) 2324–2329.
[19] L. Wang, T. Fei, Z. Lou, T. Zhang, Three-dimensional hierarchical flowerlike α-Fe_2O_3 nanostructures: synthesis and ethanol-sensing properties, ACS Appl. Mater. Interfaces 3 (2011) 4689–4694.
[20] P. Rai, J. Yoon, H. Jeong, S. Hwang, C. Kwak, J. Lee, Design of highly sensitive and selective Au@NiO yolk–shell nanoreactors for gas sensor applications, Nanoscale 6 (2014) 8292–8299.
[21] H. Kim, J. Lee, Highly sensitive and selective gas sensors using p-type oxide semiconductors: overview, Sens. Actuators B 192 (2014) 607–627.
[22] N. Cho, H. Woo, J. Lee, I. Kim, Thin-walled NiO tubes functionalized with catalytic Pt for highly selective C_2H_5OH sensors using electrospun fibers as a sacrificial template, Chem. Commun. 47 (2011) 11300–11302.
[23] X. Cao, Y. Xu, N. Wang, Facile synthesis of NiO nanoflowers and their electrocatalytic performance, Sens. Actuators B 153 (2011) 434–438.
[24] J. Ma, J. Yang, L. Jiao, Y. Mao, T. Wang, X. Duan, J. Lian, W. Zheng, NiO nanomaterials: controlled fabrication, formation mechanism and the application in lithium ion battery, CrystEngComm 14 (2012) 453–459.
[25] P. Zhang, Z. Guo, H. Liu, Submicron-sized cube-Like α-Fe_2O_3 agglomerates as an anode material for Li-ion batteries, Electrochim. Acta 55 (2010) 8521–8526.
[26] J. Lang, L. Kong, W. Wu, Y. Luo, L. Kang, Facile approach to prepare loose-packed NiO nano-flakes materials for supercapacitors, Chem. Commun. (2008) 4213–4215.
[27] C. Yuan, X. Zhang, L. Su, B. Gao, L. Shen, Facile synthesis and self-assembly of hierarchical porous NiO nano/micro spherical superstructures for high performance supercapacitors, J. Mater. Chem. 19 (2009) 5772–5777.
[28] Y. Cui, C. Wang, S. Wu, G. Liu, F. Zhang, T. Wang, Lotus-root-like NiO nanosheets and flower-like NiO microspheres: synthesis and magnetic properties, CrystEngComm 13 (2011) 4930–4934.
[29] M. Liu, Y. Wang, P. Li, Z. Cheng, Y. Zhang, M. Zhang, M. Hu, J. Li, Preparation and characterization of multilayer NiO nano-products via electrospinning, Appl. Surf. Sci. 284 (2013) 453–458.
[30] L. Wang, J. Deng, T. Fei, T. Zhang, Template-free synthesized hollow NiO-SnO_2 nanospheres with high gas-sensing performance, Sens. Actuators B 164 (2012) 90–95.
[31] Y. Zhang, W. Yang, Y. Wang, J. Jia, J. Wang, Nonenzymatic hydrogen peroxide sensor based on a glassy carbon electrode modified with electrospun PdO-NiO composite nanofibers, Microchim. Acta 180 (2013) 1085–1091.
[32] Y. Liu, G. Li, R. Mi, C. Deng, P. Gao, An environment-benign method for the synthesis of p-NiO/n-ZnO heterostructure with excellent performance for gas sensing and photocatalysis, Sens. Actuators B 191 (2014) 537–544.
[33] M. Bao, Y. Chen, F. Li, J. Ma, T. Lv, Y. Tang, L. Chen, Z. Xu, T. Wang, Plate-like p-n heterogeneous NiO/WO_3 nanocomposites for high performance room temperature NO_2 sensors, Nanoscale 6 (2014) 4063–4066.
[34] C. Feng, C. Wang, H. Zhang, X. Li, C. Wang, P. Cheng, J. Ma, P. Sun, Y. Gao, H. Zhang, Y. Sun, J. Zheng, G. Lu, Enhanced sensitive and selective xylene sensors using W-doped NiO nanotubes, Sens. Actuators B 221 (2015) 1475–1482.
[35] Y. Guan, D. Wang, X. Zhou, P. Sun, H. Wang, J. Ma, G. Lu, Hydrothermal preparation and gas sensing properties of Zn-doped SnO_2 hierarchical architectures, Sens. Actuators B 191 (2014) 45–52.
[36] Y. Lin, Y. Wang, W. Wei, L. Zhu, S. Wen, S. Ruan, Synergistically improved formaldehyde gas sensing properties of SnO_2 microspheres by indium and palladium co-doping, Ceram. Int. 41 (2015) 7329–7336.
[37] J.W. Yoon, H.J. Kim, I.D. Kim, J.H. Lee, Electronic sensitization of the response to C_2H_5OH of p-type NiO nanofibers by Fe doping, Nanotechnology 24 (2013) 444005.
[38] H. Ahn, J.H. Park, S.B. Kim, S.H. Jee, Y.S. Yoon, D.J. Kim, Vertically aligned ZnO nanorod sensor on flexible substrate for ethanol gas monitoring, Electrochem. Solid-State Lett. 13 (2010) J125–J128.
[39] P. Sahay, R. Nath, Al-doped ZnO thin films as methanol sensors, Sens. Actuators B 134 (2008) 654–659.
[40] F. Huang, W. Yang, F. He, S. Liu, Controlled synthesis of flower-like In_2O_3 microrods and their highly improved selectivity toward ethanol, Sens. Actuators B 235 (2016) 86–93.
[41] L. Yadava, R. Verma, R. Dwivedi, Sensing properties of CdS-doped tin oxide thick film gas sensor, Sens. Actuators B 144 (2010) 37–42.
[42] C. Li, X. Yin, Q. Li, T. Wang, Enhanced gas sensing properties of ZnO/SnO_2 hierarchical architectures by glucose-induced attachment, CrystEngComm 13 (2010) 1557–1563.
[43] M. Parmar, K. Rajanna, Copper (II) oxide thin film for methanol and ethanol sensing, Int. J. Smart Sens. Intell. Syst. 4 (2011) 710–725.
[44] H.J. Kim, K.I. Choi, K.M. Kim, C.W. Na, J.H. Lee, Highly sensitive C_2H_5OH sensors using Fe-doped NiO hollow spheres, Sens. Actuators B 171 (2012) 1029–1037.

Biographies

Changhao Feng received his MS degree from department of electronic sciences and technology, Heilongjiang University, China in 2012. He obtained his PhD from Jilin University of China in 2016. Now, he is a lecturer in the college of electronic and information engineering in the SouthWest University.

Xueying Kou received the B. Eng. degree in department of electronic sciences and technology in 2015. She is currently studying for her M.E. Sci. degree in College of Electronic Science and Engineering, Jilin University, China. Now, she is engaged in the synthesis and characterization of the semiconducting functional materials and gas sensors.

Bin Chen received her PhD degree in the Graduate School of Information Science and Electrical Engineering from Kyushu University (Japan) in 2014. She is now a lecturer at the College of Electronic and Information Engineering at Southwest University, and engaging in the research of chemical sensors.

Guobing Qian received B.S. degree in 2010 and P.H.D. degree in 2015 from Hunan University of Science and Technology and University of Electronic Science and Technology of China, respectively. Now he is working in Southwest University. His research interests include independent component analysis and array signal processing.

Yanfeng Sun obtained his PhD from Jilin University of China in 2007. Presently, he is working as associate professor in Electronics Science and Engineering department of Jilin University. His current research interests are nanoscience and gas sensors.

Geyu Lu received the BS degree in electronic sciences in 1985 and the MS degree in 1988 from Jilin University in China and the Dr Eng degree in 1998 from Kyushu University in Japan. Now he is a professor of Jilin University, China. He is interested in the development of functional materials and chemical sensors.